Polymer Bulletin 19, 289–295 (1988)

Polymer Bulletin

Phase separation, electrical and magnetic properties of $FeCl_3$ inhomogeneously doped PMMA

A. Tawansi*, M.A. Soliman, N. Kinawy, and S.I.M. Badr

Department of Physics, Faculty of Science, Mansoura University, Mansoura, Egypt

SUMMARY

Polymethylmethacrylate (PMMA) films doped with 1-7 wt.% $FeCl_3$ were prepared by casting method. A computer aided model was suggested for the mechanism of coursening stage of the observed spinodal phase seperation. The differential scanning calorimetry results confirmed the presence of phase separation in the studied samples. Arrhenius plots of the temperature dependence of the d.c. electrical resistivity revealed different slopes for the glassy and polymeric states. A temperature independent paramagnetic Pauli susceptibility (X) was obtained. The dependence of X on the dopant content was interpreted on the basis of nonuniform doping models.

I. INTRODUCTION

It is important to select a suitable dopant to modify the physical properties of some polymers. Therefore the doping mechanism must be understood. Iodine was mostly concerned in the previous doping studies. However recent extensive studies (1-4) considered the $FeCl_3$ dopant as an efficient electron acceptor and this was attributed to the formation of $Fe_{II}Cl_4^{2-}$. The advantage of $FeCl_3$ over I_2 as a dopant is its higher stability due to the much smaller vapour pressure (5). Most of the phase separation studies in polymers are recently focused on the form and structure of the phases that evolve during the spinodal decomposition process (6). The present work aims to characterise the morphological patterns that evolve during the late coursening stages of the spinodal phase separation in $FeCl_3$ doped PMMA. The influence of doping on the electrical resistivity and magnetic susceptibility is also studied in this work.

II. EXPERIMENTAL

The studied films were prepared by casting method as follows (7). PMMA material was dissolved in benzene. $FeCl_3+2H_2O$ was dissolved in ethyl-alcohol, and then added to the polymer solution. After the mixture attained a suitable viscosity it was cast to a glass dish, and kept in a dry atmosphere at 30°C for two weeks. Several thicknesses were available in the range of 20-80 $\pm$5 microns. The studied samples were examined by Auger spectroscopy and microprobe analyser. The differential scanning calorimetry (DSC) was carried out using a thermoanalyzer type (GDTD 16-SETARAM) with temperature range of -193 to 1200 °C, heating rate of 9°C/min., and sensitivity 2.5 μV.

* To whom offprint requests should be sent

The electrical measurements were done using standard techniques (8). The current was measured by means of an electrometer (Levell TM98P) of accuracy ±0.2%. The films were in the form of discs of 1.6 ±0.001 cm diameter. Contacts were of highly conductive silver paste with an area of 1 cm^2. A guard ring was used. The sample was short circuited for about two days, at a constant temperature (308 K), before the d.c voltage was applied. The current was measured in the steady state to avoid errors due to relaxation phenomena. The magnetic susceptibility was measured using the Faraday technique explained previously (9).

III. RESULTS AND DISCUSSION

III.a. Spinodal Phase Separation:

Fig. (1-a) presents the micrograph of the observed surface morphology during the late stages of spinodal phase separation process for PMMA film doped with 3% $FeCl_3$. Zone (A) of the micrograph exhibits the highly interconnected structure characteristic of the spinodal mechanism. Zone (B) of the micrograph implies that the structure undergoes ripening process and then it breaks into droplets that grow in time. The grown droplets are clearly shown in Fig. (1-b) The break up process of the continuous cluster to the discrete droplets may be envisaged as a percolation process by reversing the time arrow. Thus, an infinite cluster is created at the percolation threshold when the process is conceptually reversed in time (6). The element identification, using the elctron microprobe analysis, revealed that the $FeCl_3$ doped PMMA contains three possible phases, denoted by α, β and γ. The β-phase is the halide rich phase forming droplets distributed randomly in the least halide containing phase (α-phase). The γ-phase is of the highest halide content, white parts in Fig. (1-b). The γ-phase is secondary separated mainly within the β-droplets. The microprobe analysis implied that the three phases differ not only in the dopant content but also in the Fe to Cl ratio. Accordingly, the following reaction is probable (3,4):

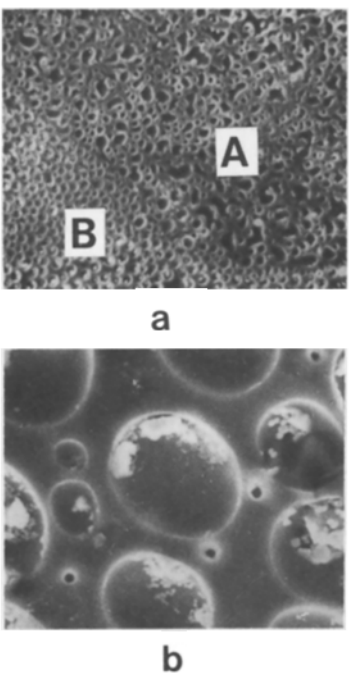

Fig. 1 Micrographs of :
a-surface morphology of PMMA doped with 3% $FeCl_3$. (X400)
b-the grown droplets. (X2000)

$$2FeCl_3 + PMMA \rightleftharpoons (PMMA)^{+}FeCl_4 + FeCl_2 \qquad (1)$$

A computer aided model is suggested to clarify the mechanism of coursening stage of spinodal phase separation process in the present case. Considering a system of continous medium (α-phase) including a certain number of circular particles (β-phase) distributed randomly in the medium. The γ-phase (dark spots in Fig. 2.a) are randomly spreaded in the system. Figs. (2.b-d) depict different successive ensembles of the suggested coursening mechanism. The physical concepts of the model can be summarized as follows. The secondary phase separation process (of γ-phase), is thought to be controlled by reaction (1). Accordingly the halide content, in

the close vicinity of γ-phase, will be changed. This results in thermodynamic fluctuations and an enhancement of the electrical polarizability within the β-phase. The activated β-phase will induce an electrostatic field. If the condition $q_i\, q_j \,/\, r_{ij}^2 <= C$ is satisfied between any two activated droplets, an electrostatic attraction will occur. This leads to a coursening process, where q_i and q_j are the effective charges on the i^{th} and j^{th} droplets respectively, separated by a distance r_{ij} and C is an adjustable parameter.

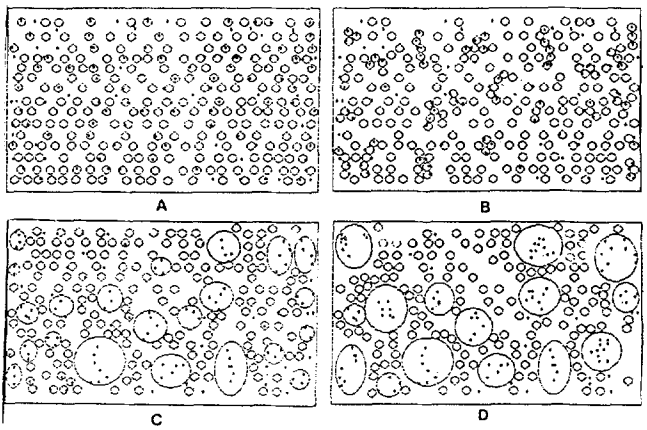

Fig.2 Simulations for the proposed mechanism of the coursening stages of the spinodal phase separation process.

III.b. Thermal Analysis:

The DSC plots for PMMA films containing 0,1,2,3,4 and 7% $FeCl_3$ are presented in Fig.(3). The T_w exotherms, within the temperature range 282-307 K, are due to the small amount of water which is always present in the conventional polymer unless it is carefully vacuum dried (10). The T_{gg} endotherms (at 306-345 K) may be arised from the rotation of the ester side-group about the C-C bond which links it to the main-chain (11). T_{g1} endotherms (at 392-404 K) can be assigned to the glass-rubber transition due to the microbrownian motion of mainchain segments. The T_{g2} endotherms (at 451-453 K) may be assigned to the glass transition of the β-microphases formed

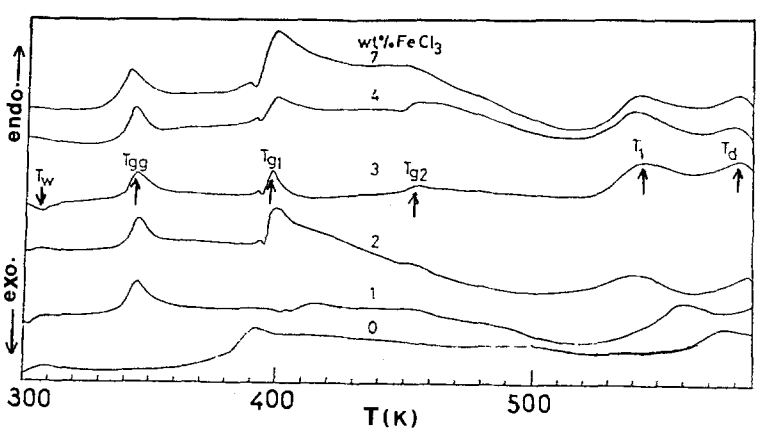

Fig.3. DSC plots of PMMA doped with 0,1,2,3,4 and 7 wt.% $FeCl_3$.

in α-phase. This assignment is favoured due to the absence of T_{g2} transition in the DSC plots of pure PMMA. At the T_1 endotherms (498-540 K) the viscoelastic fluid becomes viscous. This transition involves large scale mobility of large parts of the polymer chains. The T_d endothermic transitions (574-569 K) may refer to dissociation of the polymeric material.

III.c. Electrical Measurements:

Fig. (4-a) shows the Arrhenius plots of the d.c resistivity (ρ) of PMMA films measured in the temperature range of 300 to 453 K. The present plots can be divided into two segments separated by a transition region which contains the glass-rubber transtion temperature (T_{g1} = 392 K). It is believed that the low temperature segment corresponds to the glassy state of PMMA while the high temperature segment refers to the polymeric state.
According to the Arrhenius equation:

$$\rho = \rho_o \exp (E/KT) \qquad (2)$$

where ρ_o is constant, E - the activation energy and K is the Boltzmann's constant. Applying equation (2) for the glassy and polymeric states of Fig. (4.a) the corresponding activation energies were found to be E_g = 25.0 kcal/mol and E_p = 16.3 kcal/mol, respectively.

Fig. (4.b) depicts the Arrhenius plots for PMMA doped with 1,2,3,4 and 7 wt.% $FeCl_3$. It is clear that the resistivity temperature dependence can be divided into three segments. Each segment obeys equation (2). The low temperature segment terminates at a temperature close to T_{g2}. The second segment terminates at a temperature near to T_{g1}.

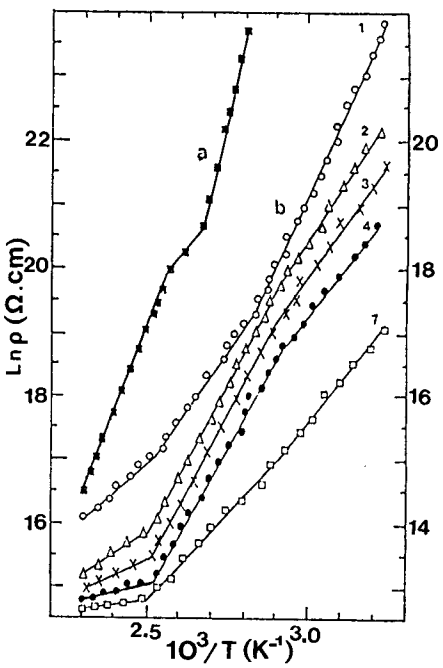

Fig. 4. Arrhenius plots for: a-PMMA (left scale), and b-1,2,3,4 and 7% $FeCl_3$ doped PMMA (right scale).

Figs. (5.a-c) show the effect of $FeCl_3$ on each of ln ρ (measured at 333, 370 and 420 K in the three segments respectively) and the activation energies E_1, E_2 and E_3 for the corresponding segments. It is clear that each of E_1, E_3, ln ρ_1 and ln ρ_3 decreases as $FeCl_3$ content increases. This is an acceptable result if we consider the assumption that $FeCl_3$ molecule inters the polymeric matrix by attaching with the ester groups existing at the main chain terminals. Thus the role of $FeCl_3$ molecules is to connect the polymeric chains to each other. Accordingly the continuous conduction paths, parallel to the long chains, predominate as $FeCl_3$ content increases; leading to a decrease in ρ and E. In Fig. (5-b) it is noteworthy to remark that as $FeCl_3$ content increases up to 4% the activation energy E_2 increases, then E_2 decreases sharply. However ln ρ_2 decreases with the increase of $FeCl_3$ content. This may be attributed to the suggestion that the charge carrier density increases with the increase of $FeCl_3$ content. It is thought that the carrier density increases to an extent sufficient to overcome the impeding effect of the increased E_2. The increase of E_2 as a function of $FeCl_3$ content

may be correlated to the structural defects and the separated microphases observed in Fig. (1).

III.d. Magnetic Susceptibility:

The magnetic susceptibility measurements, in the temperature range of 300 to 430 K, revealed a temperature independent behaviour which obeys the following equation:

$$X^P = \mu_B^2 N(E_F) \qquad (3)$$

where X^P is the Pauli susceptibility of the Fermi gas for noninteracting electrons, μ_B is the Bohr magneton and $N(E_F)$ is the density of states at the Fermi energy E_F for both spins. The results of the effect of the dopant concentration (Y) on the susceptibility are illustrated in Fig. (6). In terms of the known linear morphology of PMMA (12), the demonstration of nonuniform doping suggests a concentration gradient across the main chain diameter with the center essentially undoped (13). The present experimental results imply that in the limit of uniform doping $X^P(Y)$ remains small for $Y<Y_o$ and then rises rapidly for $Y\sim Y_o$ where Y_o signals the closing of the energy gap (14). Therefore $X^P(Y)$ can be described as a step function,

$$X^P(Y) = (X_o/2)[1+ \tanh((Y-Y_o)/\Delta Y)], \qquad (4)$$

where ΔY measures the sharpness of the step, and $X_o=\mu_B^2 N(E_F)$ is the Pauli susceptibility in the metallic state. A computer program was constructed to fit the experimental data to equation (4) using Q^2 method. The obtained results are plotted in Fig. (6) with the following parameters: $Y=0.0312$, $Y_o=0.0312$ and $X_o=4.800\times10^{-6}$ emu/mole with accuracy of $\pm0.439 \times 10^{-8}$. This curve clearly provides an adiquate description of the experimental data.

To provide a more detailed understanding of the effect of nonuniform doping a concentration gradient through the main chain (fibril) diameter might be assumed, as suggested by Epstin et al. (13) for $[CH(I_3)_Y]_X$.

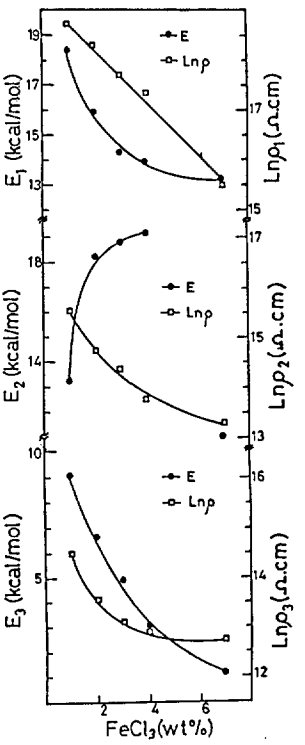

Fig. (5) The effect of dopant content on E and ln ρ for the three temperature regions.

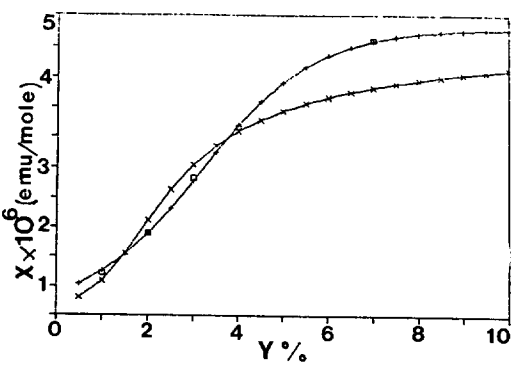

Fig. (6) The Pauli magnetic susceptibility (X) as a function of the dopant content (Y). (•) experimental points, (+) equation (4), and (x) equation (5).

The measured Pauli susceptibility X^{P}_{m} in this case is given by

$$X^{P}_{m} = (X_O/2)\{1+ \frac{Y}{2\bar{Y}} \ln \frac{\cosh [(2Y-Y_O)/\Delta Y]}{\cosh (Y_O/\Delta Y)}\}, \quad (5)$$

where $\bar{Y}$ is the average dopant concentration.
This equation is illustrated in Fig.(5) with the following parameters: $\Delta Y=0.0168, Y_O=0.0280$ and $X_O=4.8\times10^{-6}$ emu/mole with accuracy of $\pm0.7129 \times 10^{-6}$.

From the previous results one may suggest a very inhomogeneous doping in the present case in the form of random metallic like droplets. The susceptibility increases as the dopant content increases, in contrast with what one expects under homogeneous doping, viz., an effective band width that increases on doping and a X_{Pauli} that most likely decreases.

Taking the 1% $FeCl_3$ sample as an example and assuming a complete charge transfer one can expect $\sim 10^{-2}$ charge carriers per carbon atom. The observed susceptibility is only 10^{-3} that expected from such a concentration of noninteracting spins at room temperature. The small fraction of charge carriers contributing to X_{Pauli} might be taken as evidence that most of the holes created by doping from charged nonmagnetic solitons, as was suggested for doped trans-$(CH)_x$ (15), only 0.1% of the holes going into nonsoliton states and hence carrying spins. However, the susceptibility of these holes would be either Curie-like or activated, depending on their position relative to the Fermi level (16), and neither of these is observed. Thus the more traditional view, of a degenerate Fermi gas of spin-carrying holes, is in better agreement with a temperature-independent X_{Pauli}.

One can conclude from both the magnetic and transport data that the main role is due to charge carriers carrying spin, most of them delocalizing to form an impurity band with a Pauli susceptibility and a conductivity that involves hopping between random droplets..

REFERENCES

1. A.Pron, D.Billaud, J.Kulnewicz, C.Budnowski, J.Przylinski and J.Suqualski Mat. Res. Bull. 16, 1229(1981)
2. A.Pron, D.Billaud, P.Bernier and S.Lefrant, Polymer Prep. 23,96(1982)
3. H.Shirakawa and T.Kobayashi, J. de Physique C3,3(1983)
4. H.Kunonda, J.Ikemoto, K.Asakura, H.Ishii, H.Shirakawa, T.Kobayashi, H.Oyanagi and M.Matsushita, Solid State Commun. 46, 235(1983)
5. F.Beniere and S.Pekker, Solid State Commun. 57, 835(1986)
6. S.Reich, Phys. Lett., 114A, 90(1986)
7. A.Tawansi, M.D.Migahed and M.I.A.El-Hamid, J.Polym.Sci. B:Polym.Phys.Ed., 24, 2631(1986)
8. A.Tawansi, M.D.Migahed and M.I.A.El-Hamid, Phys. D: Appl.Phys., P20, 766(1987)
9. A.Tawansi, in "Magnetic Properties of Some Compounds and Alloys Containing Rare Earth and Uranium", Ph.D. Thesis, Moscow State University (1977).
10. P.Hedvig, in "Dielectric Spectroscopy of Polymers", Adam Hilger Ltd., Bristol, 76(1977)
11. G.P.Mikhailov, Uszpehi Khimi, 24, 875(1955)
12. A.Strepikheyev, V.Derevitskaya and G.Slonimsky, in "A First Course in Polymer Chemistry", Mir Publishers, Moscow, 354(1971)

13. A.J.Epstein, H.Rommelmann, M.A.Druy, A.J.Heeger and A.G.MacDiarmid, Solid State Commuen., 38, 683(1981)
14. J.J.Ritsko, E.J.Mele, A.J.Heeger, A.G.MacDiarmid and M.Ozaki, Phys.Rev.Lett., 44, 1351(1980)
15. I.B.Goldberg, H.R.Crowe, P.R.Newman, A.J.Heeger and A.G.MacDiarmid, J.Chem.Phys., 70, 1132(1979)
16. Y.Tomkiewicz, T.D.Schultz, H.B.Broom, T.C.Clarke and G.B.Street, Phys.Rev.Lett., 43, 1532(1979)

Accepted December 4, 1987 C